Supporting Information

Homogeneous Catalytic System for Photoinduced Hydrogen Production Utilizing Iridium and Rhodium Complexes

Eric D. Cline, Samantha E. Adamson, Stefan Bernhard*

Contribution from the Department of Chemistry, Princeton, University, Frick Laboratory, Princeton, New Jersey 08544

I. Synthesis Experimental Procedures

Spectroscopic characterization of [Ir(ppy)$_2$(bpy)](PF$_6$), [Ir(f-mppy)$_2$(bpy)](PF$_6$), [Ir(ppy)$_2$(dmbbpy)](PF$_6$), [Ir(ppy)$_2$(dtbbpy)](PF$_6$), and [Ir(df-CF$_3$ppy)$_2$(dtbbpy)](PF$_6$) was previously reported.[1-5]

Titration of Hydrazine Equivalency for {Rh(N^N)$_3$]$^{3+}$ Synthesis. To RhCl$_3$•2H$_2$O (172 mg, 702 µmol) and bpy (361 mg, 2.49 mmol) was added EtOH (7 ml) and H$_2$O (7 ml). Divided the solution evenly between seven reaction vials, and then heated the reactions at 80ºC for 15 min. Added the appropriate amount (0, 20, 40, 60, 80, 100, or 200 µL) of a 1M solution of hydrazine in EtOH/H$_2$O to each reaction, and then continued heating at 80ºC for an additional 1 h. Following counter-ion metathesis with NH$_4$PF$_6$, the products were isolated by filtration, washed with water and EtOH, and dried under high vacuum overnight. The crude products were characterized by ^{1}H-NMR (500 MHz, Acetone-*d6*) to determine the amount of conversion of **[**Rh(bpy)$_2$Cl$_2$]$^+$ to [Rh(bpy)$_3$]$^{3+}$ as a result of added hydrazine. An overlay of the aromatic regions for the ^{1}H-NMR results is presented below as Figure S1. Titration of the hydrazine equivalency proves that under aerobic conditions the reaction is not catalytic through self-redox, requiring a full equivalent of hydrazine to reduce **[**Rh(bpy)$_2$Cl$_2$]$^+$ and promote ligand labilization. Subsequent reoxidation of [Rh(bpy)$_2$]$^+$ by dissolved oxygen would promote association of the third bpy ligand to form [Rh(bpy)$_3$]$^{3+}$.

Synthesis of 5,5'-difluoro-2,2'-bipyridine (dfbpy). To NiCl$_2$ (6.73 g, 28.4 mmol) and PPh$_3$ (23.5 g, 89.6 mmol) was added DMF (250 ml), and the reaction was heated for 1.5 h (50ºC, N2, mag stir). To the reaction was added Zn powder (1.85 g, 28.4 mmol), and the reaction was continued for 2.5 h (previous conditions). To the reddish brown reaction mixture was added 2-bromo-5-fluoropyridine (5.0 g, 28.4 mmol) in DMF (20 ml), and the reaction was allowed to run overnight (previous conditions). Poured cooled reaction mixture into conc. NH$_4$OH (400 ml) and stirred for 1.5 h at RT. Extracted with EtOAc (2 x 350 ml), then concentrated the combined organic to 200 ml by rotary evaporation. Extracted with conc. HCl (3 x 50 ml), washed the combined aqueous with EtOAc (100 ml), neutralized to pH 9, and extracted with EtOAc (3 x 150 ml). Washed combined organic with water (100 ml) and brine (100 ml), dried Na$_2$SO$_4$, and concentrated to dryness in vacuo. A recrystalization from EtOH yielded dfbpy as yellow needle-like crystals (2.21 g, 80% yield).

^{1}H-NMR (500 MHz, CDCl$_3$): δ 8.47 (d, 2 H, *J* = 2.5), 8.35 (dd, 2H, *J* = 8.5, 4.5), 7.49 (td, 2H, *J* = 8.5, 2.5). ^{13}C-NMR (125 MHz, CDCl$_3$): δ 160.0 (d, *J* = 258), 151.7 (d, *J* = 4), 137.5 (d, *J* = 24), 124.0 (d, *J* = 18), 122.3 (d, *J* = 5). ^{19}F-NMR (300 MHz, CDCl$_3$): δ -127.8 (dd, *J* = 8.0, 5.5). High Res. MS (m/e, ESI+): Calcd for C$_{10}$H$_6$F$_2$N$_2$ 192.0499, Found 192.0493.

Synthesis of [(2,2'-bipyridine)-*bis*-(2-(4-methoxy-phenyl)-5-methyl-pyridine)-iridium(III)] hexafluorophosphate. Cleaved [(MeO-mppy)$_2$Ir-m-Cl]$_2$ with bpy according to general procedure.[1]

1. Lowry, M. S.; Goldsmith, J. I.; Slinker, J. D.; Rohl, R.; Robert A. Pascal, J.; Malliaras, G. G.; Bernhard, S. *Chem. Mater.* **2005**, *17*, 5712 – 5719.
2. Lowry, M. S.; Hudson, W. R.; Pascal, R. A.; Bernhard, S. *J. Am. Chem. Soc.* **2004**, *126*, 14129-14135.
3. Slinker, J. D.; Gorodetsky, A. A.; Lowry, M. S.; Wang, J.; Parker, S.; Rohl, R.; Bernhard, S.; Malliaras, G. G. *J. Am. Chem. Soc.* **2004**, *126*, 2763-2767.
4. Goldsmith, J. I.; Hudson, W. R.; Lowry, M. S.; Anderson, T. H.; Bernhard, S. *J. Am. Chem. Soc.* **2005**, *127*, 7502-7510.
5. Ohsawa, Y.; Sprouse, S.; King, K. A.; DeArmond, M. K.; Hanck, K. W.; Watts, R. J. *J. Phys. Chem.* **1987**, *91*, 1047-1054.

Purified by vapor diffusion recrystalization (ACN/Et$_2$O) to give [Ir(bpy)(MeO-mppy)$_2$](PF$_6$) as orange cubic crystals in 85% yield.

^{1}H-NMR (500 MHz, Acetone-d_6): δ 8.81 (d, 2 H, J = 8.5), 8.29 (t, 2 H, J = 8.0), 8.16 (d, 2 H, J = 5.5), 7.99 (d, 2 H, J = 8.5), 7.80 (d, 2 H, J = 8.5), 7.72 (d, 2 H, J = 8.5), 7.71 (dd, 2 H, J = 8.0, 5.5), 7.53 (s, 2 H), 6.63 (dd, 2 H, J = 8.5, 2.5), 5.81 (d, 2 H, J = 2.5), 3.58 (s, 6 H), 2.09 (s, 6 H). ^{13}C-NMR (125 MHz, Acetone-d_6): δ 166.1, 161.8, 157.0, 153.0, 151.7, 149.1, 140.4, 129.4, 125.7, 118.1, 108.1, 55.0, 17.9. Elem. Anal. Calcd for C$_{36}$H$_{32}$IrN$_4$O$_2$(PF$_6$): C, 48.59; H, 3.62; N, 6.30. Found: C, 48.37; H, 3.47; N, 6.27.

Synthesis of [(2,2'-bipyridine)-*bis*-(2-(2,4-difluoro-phenyl)-5-trifluoromethyl-pyridine)-iridium(III)] hexafluorophosphate. Cleaved [(df-CF$_3$ppy)$_2$Ir-m-Cl]$_2$ with bpy according to general procedure.[1] Purified by column chromatography (silica, 0-25% ACN/DCM) and vapor diffusion recrystalization (acetone/pentane) to give [Ir(bpy)(df-CF$_3$ppy)$_2$](PF$_6$) as yellow needle-like crystals in 44% yield.

^{1}H-NMR (500 MHz, Acetone-d_6): δ 8.89 (d, 2 H, J = 8.5), 8.62 (dd, 2 H, J = 8.5, 2.5), 8.41 (dd, 2 H, J = 8.0, 1.0), 8.40 (td, 2 H, J = 8.0, 1.0), 8.31 (dd, 2 H, J = 5.5, 1.0), 7.98 (d, 2 H, J = 1.0), 7.80 (ddd, 2 H, J = 7.5, 5.5, 1.0), 6.86 (ddd, 2 H, J = 12.5, 9.5, 2.0), 5.96 (dd, 2H, J = 8.5, 2.0). ^{13}C-NMR (125 MHz, Acetone-d_6): δ 168.7 (d, J = 7.0), 165.5 (dd, J = 258.5, 12.5), 163.4 (dd, J = 261.5, 13.0), 156.9, 156.1 (d, J = 7.0), 152.6, 147.1 (dd, J = 9.5, 4.5), 141.6, 138.3, 130.2, 127.8 (dd, J = 4.0, 2.5), 126.4 (q, J = 34.5), 126.3, 124.9 (d, J = 21.0), 124.2, 122.0, 115.5 (d, J = 21.0), 100.3 (t, J = 7.0). ^{19}F-NMR (300 MHz, Acetone-d_6): δ -64.0, -73.1 (d, J = 750 Hz), -105.1, -108.4. Elem. Anal. Calcd for C$_{34}$H$_{18}$IrF$_{10}$N$_4$(PF$_6$): C, 40.44; H, 1.80; N, 5.55. Found: C, 39.81; H, 2.18; N, 4.61.

Synthesis of [(1,2-bis-(diphenylphosphino)-ethane)-*bis*-(2-phenyl-pyridine)-iridium(III) hexafluorophosphate. Cleaved [(ppy)$_2$Ir-m-Cl]$_2$ with dppe according to literature procedure.[1] Purified by trituration with 1:1 Et$_2$O/acetone to yield [Ir(dppe)(ppy)$_2$](PF$_6$) as a pale yellow powder in 73% yield.

^{1}H-NMR (500 MHz, DMSO-d_6): δ 7.85-7.75 (m, 8 H), 7.57 (t, 2 H, J = 7.5), 7.45 (t, 2 H, J = 7.0), 7.34 (t, 4 H, J = 7.0), 7.08 (t, 2 H, J = 7.0), 7.05 (t, 2 H, J = 7.0), 6.96 (t, 2 H, J = 7.5), 6.91 (t, 4 H, J = 7.0), 6.69 (t, 4 H, J = 8.5), 6.38 (t, 2 H, J = 6.5)), 6.34 (dd, 2 H, J = 7.0, 3.5), 5.50, (s, 2H), 3.91 (d, 1 H, J = 10.0), 3.85 (d, 1 H, J = 10.0), 2.88 (d, 2 H, J = 9.0). ^{13}C-NMR (125 MHz, DMSO-d_6): δ 158.6 (d, J = 87.5), 158.5 (d, J = 87.5), 145.2, 139.2, 134.42 (d, J = 4.5), 134.38 (d, J = 4.5), 133.6, 133.4, 133.2, 132.7, 131.2, 130.80 (d, J = 4.0), 130.76 (d, J = 4.0), 130.23 (d, J = 5.0), 130.19 (d, J = 5.0), 129.73 (d, J = 4.5), 129.69 (d, J = 4.5), 126.4, 124.7, 124.3, 122.1, 27.6 (J, J = 43.5). Elem. Anal. Calcd for C$_{48}$H$_{40}$IrN$_2$P$_2$(PF$_6$): C, 55.22; H, 3.86; N, 2.68. Found: C, 54.99; H, 4.01; N, 2.63.

Synthesis of [(4,4'-di-*tert*-butyl-2,2'-bipyridine)-*bis*-(2-(4-methoxy-phenyl)-5-methyl-pyridine)-iridium(III)] hexafluorophosphate. Cleaved [(MeO-mppy)$_2$Ir-m-Cl]$_2$ with dtbbpy according to general procedure.[1] Purified by column chromatography (silica, 0-20% ACN/DCM) and vapor diffusion recrystalization (acetone/pentane) to give [Ir(dtbbpy)(MeO-mppy)$_2$](PF$_6$) as a yellow powder in 82% yield.

^{1}H-NMR (500 MHz, Acetone-d_6): δ 8.85 (d, 2 H, J = 2.0), 8.05 (d, 2 H, J = 6.0), 7.98 (d, 2 H, J = 8.0), 7.79 (d, 2 H, J = 8.5), 7.73 (dd, 2 H, J = 6.0, 2.0), 7.72 (dd, 2 H, J = 8.5, 1.0), 7.41 (d, 2 H, J = 1.0), 6.62 (dd, 2 H, J = 8.5, 2.5), 5.80 (d, 2 H, J = 2.5), 3.58 (s, 6 H), 2.08 (s, 6 H), 1.43 (s, 18 H). ^{13}C-NMR (125 MHz, Acetone-d_6): δ 164.8, 161.9, 156.9, 153.6, 151.3, 148.8, 140.1, 137.9, 133.0, 127.0, 126.4, 122.8, 119.6, 117.9, 108.1, 55.0, 36.9, 30.5, 18.0. MS (*m/e*, ESI): 859 (100, M$^+$ + H). Elem. Anal. Calcd for C$_{44}$H$_{48}$IrN$_4$O$_2$(PF$_6$): C, 52.74; H, 4.83; N, 5.59. Found: C, 52.34; H, 4.68; N, 5.48.

Synthesis of [*tris*-(2,2'-bipyridine)-rhodium(III)] *tris*-hexafluorophosphate. Based upon a literature procedure.[6] To RhCl$_3$•2H$_2$O (202 mg, 808 µmol) and bpy (378 mg, 2.42 mmol) was added EtOH (10 ml) and H$_2$O (10 ml). Heated reaction at 80ºC for 15 min. Added 0.8 ml of a 1M solution of hydrazine in EtOH/H$_2$O. Continued heating at 80ºC for an additional 1 h. Concentrated to 10 ml volume by rotary evaporation, added NH$_4$PF$_6$ (1.0 g in H$_2$O), isolated solids by vac filtration, washed water, and dried under high vac overnight. Purified by vapor diffusion recrystalization (ACN/Et$_2$O) to give [Rh(bpy)$_3$](PF$_6$)$_3$ as a white cubic crystal in 69% yield.

^{1}H-NMR (500 MHz, Acetone-d_6): δ 9.04 (d, 6 H, J = 8.0), 8.62 (dd, 6 H, J = 8.0, 7.0), 8.26 (d, 6 H, J = 6.0), 7.89 (dd, 6 H, J = 7.0, 6.0).

---

6   Hillis, J. E.; DeArmond, M. K. *J. Lumin.* **1971**, *4*, 273-290.

Synthesis of [*tris*-(5,5'-dimethoxy-2,2'-bipyridine)-rhodium(III)] *tris*-hexafluorophosphate.
Synthesized in the same manner as [Rh(bpy)$_3$](PF$_6$)$_3$ using dMeObpy. Purified by column chromatography
(aluminum oxide, 0-2% H$_2$O/acetone) to give [Rh(dMeObpy)$_3$](PF$_6$)$_3$ as a white solid in 25% yield.
^{1}H-NMR (500 MHz, Acetone-d_6): δ 8.83 (d, 6 H, J = 9.0), 8.17 (d, 6 H, J = 9.0), 7.60 (s, 6 H), 3.94 (s, 18
H). ^{13}C-NMR (125 MHz, Acetone-d_6): δ 159.9, 148.6, 140.5, 127.7, 126.9, 57.6. Elem. Anal. Calcd for
C$_{36}$H$_{36}$N$_6$O$_6$Rh(PF$_6$)$_3$: C, 36.44; H, 3.06; N, 7.08. Found: C, 39.36; H, 3.52; N, 6.32.

Synthesis of [*tris*-(5,5'-difluoro-2,2'-bipyridine)-rhodium(III)] *tris*-hexafluorophosphate. Synthesized
in the same manner as [Rh(bpy)$_3$](PF$_6$)$_3$ using dfbpy. Purified by column chromatography [silica, 0-5%
H$_2$O (5wt% NH$_4$PF$_6$)/ACN] to give [Rh(dfbpy)$_3$](PF$_6$)$_3$ as a yellow solid in 60% yield.
^{1}H-NMR (500 MHz, CDCl$_3$): δ 9.11 (dd, 6 H, J = 9.0, 4.0), 8.56 (dd, 6H, J = 9.0, 7.0), 8.34 (s, 6H). [13]C-
NMR (125 MHz, CDCl$_3$): δ 162.5 (d, J = 262), 152.7, 142.4 (d, J = 34), 132.1 (d, J = 19), 130.2 (d, J = 9).
^{19}F-NMR (300 MHz, CDCl$_3$): δ -72.8 (d, J = 750 Hz), -112.9. Elem. Anal. Calcd for C$_{30}$H$_{18}$F$_6$N$_6$Rh(PF$_6$)$_3$:
C, 32.34; H, 1.63; N, 7.54. Found: C, 31.53; H, 1.64; N, 7.49.

Synthesis of a tertiary-amine stabilized Rh colloid. Synthesized according to literature procedure.[7] To
RhCl$_3$•2H$_2$O (24.5 mg, 100 µmol) in water (5 mL) was added a solution of trioctylamine (141.5 mg,
400 µmol) in CHCl$_3$ (5 mL), and the biphasic mixture was stirred vigorously overnight at RT under H$_2$ (2
atm). Removed organic solvent by rotary evaporation. Transferred the aqueous portion with large
particulate metal to a 100 mL volumetric flask and then diluted to volume with water for a 1.0 mM aqueous
solution of trioctylamine-Rh colloid.

Synthesis of a polymer stabilized Rh colloid. Synthesized according to literature procedure.[8] To
RhCl$_3$•2H$_2$O (8.4 mg, 33 µmol) in MeOH (25 mL) was added a solution of polyvinylpyrrolidone (MW
8000, 150 mg) in MeOH (20 mL), and the reaction was refluxed for 30 min. To the refluxing reaction was
slowly added a solution of NaOH (7.0 mg, 0.18 mmol) in MeOH (5 mL), and the reaction was refluxed for
an additional 5 min. Concentrated the dark brown solution to dryness by rotary evaporation. Transferred
the colloid to a 5 mL volumetric flask using water and then diluted to volume with water for a 6.6 mM
aqueous solution of PVP-Rh colloid.

II. Photoreaction Experimental Procedures and Results

Photoreaction Specifications. Reactions were conducted in 40 ml EPA vials capped with a homemade
vial closure assembly equipped with silicone rubber septa (Restek Ice Blue) for needle access and a
differential pressure transducer (Omega PX-138-015D5V) for real-time analysis of gas production. The
transducers have an operating range of ±15 psi with an accuracy of ±0.015 psi, and they are driven in
parallel at 8 V using a variable power supply (Temna 72-2005). Pressure data are collected using a PC
interface designed in LabView. Pressure data are corrected for temperature and pressure variations of the
external environment using a reference sample without catalyst.

Samples were evaluated using a home-built 16-sample photoreactor. Bottom illumination is provided by
Luxeon V Dental Blue LEDs (LXHL-LRD5) with collimating optics (Fraen FHS-HNB1-LL01-H) mounted
on a copper plate fitted to a water-cooled aluminum base. The LEDs are driven two in series at 700 mA
using a Xitanium Driver (Future Electronics), providing a total output power of 500 ± 50 mW at 460 ± 10
nm. The entire setup is agitated at 150 ppm on an orbital shaker (IKA KS-260). The samples were then
subjected to continuous photolysis until hydrogen production had slowed.

Photoreaction Analysis. For early studies, gas composition was determined by gas chromatograph (GC)
analysis on a Perkin-Elmer 3920 chromatograph with a 13x80/100 mesh mol sieve column (Alltech),
thermal conductivity detector, and argon carrier gas. The instrument was calibrated with H$_2$/Ar mixtures
before each use. Reaction overpressure was released by using a canula to transfer it into an inverted water-
filled graduated buret, and then the headspace was sampled directly in 1 mL volumes. For later studies, gas
composition was determined by mass spectrometry using a Stanford Research Systems QMS200 Gas
Analyzer residual gas analyzer (RGA) with nitrogen carrier gas, custom-made sample chamber, and
Labview interface. The instrument was calibrated with commercial H$_2$/Ar mixtures before each use. The
pressurized reaction headspace was sampled directly in approximately 0.3 mL volumes. H$_2$ percentage was
determined by averaging the results of three samples of the reaction headspace gas. Reaction kinetics was
obtained from the real-time pressure data by normalized for H$_2$ production following endpoint analysis of

[7] Yonezawa, T.; Tominaga, T.; Richard, D. *J. Chem. Soc. Dalton Trans.* **1996**, 783 - 789.

[8] Wang, Q.; Liu, H.; Han, M.; Li, X.; Jiang, D. *J. Mol. Catal. A: Chem.* **1997**, *118*, 145-151.

the reaction headspace. Additionally, the plots can be normalized using TON for the catalyst of interest to allow for comparison between reactions of different catalyst concentrations.

The catalytic rate plot was obtained from the TON kinetic plot by smoothing with an adjacent point average to reduce instrument noise and then taking the first derivative of the smoothed data. The maximum PS catalytic rate from these plots was converted to quantum yield (QY) (0.5 H_2 per photon absorbed) according to equations S1-S3. The photon flow (Φ_P) (Equation S1) is calculated from the rated power (P) of the LED and collimating optics (500 ± 50 mW) at the max wavelength ($\lambda = 460 \pm 10$ nm). The photons absorbed (Equation S2) is calculated from the molar absorptivity of the PS (460 nm, $\varepsilon = 553 \pm 5$ M^{-1} cm^{-1} for [Ir(f-mppy)$_2$(dtbbpy)](PF$_6$) in 80% THF/H$_2$O), pathlength ($l = 2.0 \pm 0.1$ cm), and PS concentration (C) for the individual reaction. The QY (Equation S3) can then be calculated using the maximum catalytic rate (TON per time), PS concentration (C), and reaction volume (V).

$$\Phi_P = (P * \lambda) / (h * c) \qquad \text{(S1)}$$

$$\text{photons absorbed} = \Phi_P (1 - 10^{-\varepsilon Cl}) \qquad \text{(S2)}$$

$$QY = \text{rate} * C * V * N_A / \text{photons absorbed} \qquad \text{(S3)}$$

Catalyst System Comparison. To two EPA vials was added 1 mL of a 10.0 mM solution of either [Co(bpy)$_3$]Cl$_2$ or [Rh(bpy)$_3$](PF$_6$)$_3$ in ACN. To one vial of each type was added 1 mL of a 10.0 mM solution of either [Ir(ppy)$_2$(bpy)](PF$_6$) or [Ru(bpy)$_3$](PF$_6$)$_2$ in ACN. Concentrated to dryness by rotary evaporation soon thereafter. Immediately preceding photolysis, added 10 ml of a 0.6 M solution of triethanolamine (TEOA) in 50% acetonitrile-water (ACN-H$_2$O). Evaluated according to the general procedure above and analyzed headspace by GC. The kinetics curves were fit with a unimolecular exponential decay function H$_2$ (t) = α (1 - e$^{-t/t}$), where α is the net hydrogen produced and t is the decay lifetime. Both experiments had an induction period requiring the graphs to be offset for purposes of the decay fit. The kinetics plot is presented in the text as Figure 3. Catalytic rate and decay fit plots are presented below in Figure S2.

TEOA/ACN/H$_2$O Condition Optimization. To six EPA vials was added 1 mL of a solution that is 10.0 mM of [Ir(ppy)$_2$(bpy)](PF$_6$) and [Rh(bpy)$_3$](PF$_6$)$_3$ in ACN. Concentrated to dryness by rotary evaporation soon thereafter. Immediately preceding photolysis, added 10 ml of a 0.6 M solution of TEOA in the appropriate ACN-H$_2$O mixture (40%, 60%, 80%, 90%, 95%, or 100% ACN). Evaluated according to the general procedure above and analyzed headspace by GC. The kinetics traces and a graph illustrating the endpoint H$_2$ results by solvent composition are presented below in Figure S3.

Structure Activity Relationship. For this study, synthesized seven PSs of the form [Ir(C^N)$_2$(N^N)](PF$_6$) where C^N is ppy, f-mppy, MeO-mppy, or df-CF$_3$ppy when N^N is bpy and N^N is bpy, dtbbpy, dmbpy, or dppe when C^N is ppy. Synthesized four ERs of the form [Rh(N^N)$_3$](PF$_6$)$_3$ where N^N is bpy, dfbpy, dMeObpy, or dtbbpy. Prepared the samples by distributing 1 mL of stock solutions (10 mM in ACN) of the seven PSs and four ERs into EPA vials in a 7x4 array. Concentrated to dryness by rotary evaporation soon thereafter. Immediately preceding photolysis, added 10 ml of a 0.6 M solution of TEOA in 90% ACN-H$_2$O. Evaluated according to the general procedure above and analyzed headspace by GC. The kinetics curves are presented below in Figure S7. A three-dimensional chart of the combinatorial screening endpoint results is presented in the article text as Figure 4.

Cyclometallating Ligand Evaluation. For this study, synthesized four PSs of the form [Ir(C^N)$_2$(dtbbpy)](PF$_6$), where C^N is ppy, f-mppy, MeO-mppy, or df-CF$_3$ppy, for evaluation with the best ER, [Rh(dtbbpy)$_3$](PF$_6$)$_3$. Prepared the samples by weighing 10 μmol of each PS into an EPA vial before adding 10 mL of a solution that is 1.0 mM of ER and 0.6 M of TEOA in 90% ACN-H$_2$O. Evaluated according to the general procedure above and analyzed headspace by GC. The kinetics curves are presented in the text as Figure 5.

Sacrificial Reductant Evaluation. To three EPA vials was added 1 mL of a solution that is 1.0 mM of [Ir(f-mppy)$_2$(dtbbpy)](PF$_6$) and [Rh(dtbbpy)$_3$](PF$_6$)$_3$ in ACN. Concentrated to dryness by rotary evaporation soon thereafter. Immediately preceding photolysis, added 10 ml of a 0.6 M solution of the appropriate sacrificial reductant (TEOA, TEA, or DMA) in 90% ACN-H$_2$O. Evaluated according to the general procedure above and analyzed headspace by RGA. The kinetics curves are presented in the text as Figure 6.

Solvent Evaluation. To three EPA vials was added 1 mL of a solution that is 1.00 mM of [Ir(f-mppy)$_2$(dtbbpy)](PF$_6$) and [Rh(dtbbpy)$_3$](PF$_6$)$_3$ in ACN. Concentrated to dryness by rotary evaporation soon thereafter. Immediately preceding photolysis, added 10 ml of a 0.6 M solution of TEOA in the appropriate 90% solvent-water mixture (ACN, DMF, or THF). Evaluated according to the general procedure above and analyzed headspace by RGA. The kinetics curves are presented in the text as Figure 6.

TEA/THF/H$_2$O Condition Optimization. To an EPA vial was added the appropriate volume of a solution that is 1.0 mM of [Ir(f-mppy)$_2$(dtbbpy)](PF$_6$) and [Rh(dtbbpy)$_3$](PF$_6$)$_3$ and 0.6 M of TEA in either 50% or 99.9% THF-water to make a 10 mL reaction with the desired THF-water mixture (50, 70, 75, 80, 90, 95, or 99.9%). Evaluated according to the general procedure above and analyzed headspace by RGA. The kinetic and catalytic rate plots are presented below as Figure S8. The data is also presented in the text as Table 1.

TEA Concentration Dependence. To five EPA vials was added 1 mL of a 1.00 mM solution of [Ir(f-mppy)$_2$(dtbbpy)](PF$_6$) in ACN and 1 mL of a 1.00 mM solution of [Rh(dtbbpy)$_3$](PF$_6$)$_3$ in ACN. Concentrated to dryness by rotary evaporation soon thereafter. Immediately preceding photolysis, added 10 mL of a solution of the appropriate concentration of TEA (0.6, 0.3, 0.09, 0.06, or 0.03 M) in 80% THF-water. Evaluated according to the general procedure above and analyzed headspace by RGA. The kinetics curves are presented in the text as Figure 8.

Catalyst Concentration Optimization. To five EPA vials was added the appropriate volume (1.5, 2.25, 3.0, 3.75, or 4.5 mL) of a solution that is 0.334 mM of [Rh(dtbbpy)$_3$](PF$_6$)$_3$ and 0.6 M of TEA in 80% THF-water. To one of each type of vial was added the appropriate volume (1.5, 2.25, 3.0, 3.75, or 4.5 mL) of a solution that is 0.336 mM of [Ir(f-mppy)$_2$(dtbbpy)](PF$_6$) and 0.6 M of TEA in 80% THF-water. Filled each vial to 10 mL total volume with 0.6 M solution of TEA in 80% THF-water. Evaluated according to the general procedure above and analyzed headspace by RGA. The kinetics curves are presented below as Figure S9. The endpoint results, catalytic rates and QY are reported in Table S1. The Rh and Ir TON are presented in a 3-D graph along with the kinetic plot and rate plot for the best performing reaction in the text in Figure 7.

[Rh(N^N)$_3$](PF$_6$)$_3$ and [Rh(N^N)$_2$Cl$_2$](PF$_6$) Comparison. To two EPA vials was added 1 mL of a 1.00 mM solution of [Ir(f-mppy)$_2$(dtbbpy)](PF$_6$) in ACN, then added 955 µL of a 1.05 mM solution of [Rh(dtbbpy)$_2$Cl$_2$](PF$_6$)$_3$ in ACN or 1 mL of a 1.00 mM solution of [Rh(dtbbpy)$_3$](PF$_6$)$_3$ in ACN. To two EPA vials was added 1 mL of a 1.00 mM solution of [Ir(ppy)$_2$(bpy)](PF$_6$) in ACN, then added 955 µL of a 1.05 mM solution of [Rh(bpy)$_2$Cl$_2$](PF$_6$)$_3$ in ACN or 990 µL of a 1.01 mM solution of [Rh(bpy)$_3$](PF$_6$)$_3$ in ACN. Concentrated to dryness by rotary evaporation soon thereafter. Immediately preceding photolysis, added 10 mL of a 0.6 M solution of TEA in 80% THF-water. Evaluated according to the general procedure above and analyzed headspace by RGA. The kinetics curves are presented below as Figure S4.

Rh Colloid Test. To five EPA vials was added 5 mL of a solution that is 0.0502 mM [Ir(f-mppy)$_2$(dtbbpy)](PF$_6$) and 0.6M TEA in 80% THF-water. To the first vial was added 5 mL of a solution that is 0.0104 mM [Rh(dtbbpy)$_3$](PF$_6$)$_3$, 0.0502 mM [Ir(f-mppy)$_2$(dtbbpy)](PF$_6$), and 0.6 M TEA in 80% THF-water. To the second vial was added 5 mL of a solution that is 0.010 mM PVP-Rh colloid, 0.0502 mM [Ir(f-mppy)$_2$(dtbbpy)](PF$_6$), and 0.6 M TEA in 80% THF-water. To the third vial was added 5 mL of a solution that is 0.010 mM trioctylamine-Rh colloid, 0.0502 mM [Ir(f-mppy)$_2$(dtbbpy)](PF$_6$), and 0.6 M TEA in 80% THF-water. To the fourth vial was added 5 mL of a solution that is 0.0100 mM RhCl$_3$•2H$_2$O, 0.0502 mM [Ir(f-mppy)$_2$(dtbbpy)](PF$_6$), and 0.6 M TEA in 80% THF-water. To the fifth vial was added an additional 5 mL of a solution that 0.0502 mM [Ir(f-mppy)$_2$(dtbbpy)](PF$_6$) and 0.6 M TEA in 80% THF-water. Evaluated according to the general photolysis procedure above and analyzed headspace by RGA. At the reaction endpoint, Ir-PS with [Rh(dtbbpy)$_3$](PF$_6$)$_3$ produced 1075 µmols H$_2$; with trioctylamine-Rh colloid produced 7 µmols H$_2$; with PVP-Rh colloid produced 8 µmols H$_2$; with RhCl$_3$•2H$_2$O colloid produced 23 µmols H$_2$; and without WRC produced 7 µmols H$_2$.

Mercury Poison Test. To five EPA vials was added 10 mL of a solution that is 0.0500 mM [Ir(f-mppy)$_2$(dtbbpy)](PF$_6$), 0.0499 mM [Rh(dtbbpy)$_3$](PF$_6$)$_3$, and 0.6 M TEA in 80% THF-water. To four of the vials was added mercury (1.0 g, 5 mmol), and the reactions were allowed to vigorously stir in the dark for 1 hour. Filtered to remove mercury from two of the vials and transferred the filtrate to new EPA vials. Placed one of the pretreated vials and one of the mercury vials on a two-position stirring photoreactor with magnetic stirring at 1200 rpm and forced air cooling but no reference vial for baseline correction. Placed the other three reactions on the normal photoreactor with orbital shaking at 150 rpm. Evaluated according to the general photolysis procedure above and analyzed headspace by RGA. The kinetic plots are in the text as Figure 11.

Quantitative CS$_2$ Poison Test. To seven EPA vials was added the appropriate volume (0, 1, 2, 3, 4, 5, or 10 mL) of a solution that is 0.50 mM CS$_2$, 0.0500 mM [Ir(f-mppy)$_2$(dtbbpy)](PF$_6$), 0.0499 mM [Rh(dtbbpy)$_3$](PF$_6$)$_3$, and 0.6 M TEA in 80% THF-water. Diluted each vial to 10 mL total volume with a solution that is 0.0500 mM [Ir(f-mppy)$_2$(dtbbpy)](PF$_6$), 0.0499 mM [Rh(dtbbpy)$_3$](PF$_6$)$_3$, and 0.6 M TEA in 80% THF-water. Evaluated according to the general photolysis procedure above and analyzed headspace by RGA. The kinetic plots are presented below as Figure S5 and a plot of endpoint results per equivalent of CS$_2$ is included in the text as Figure 12.

Isotope Labeling Study. To two EPA vials was added 1 mL of a 1.00 mM solution of [Ir(f-mppy)$_2$(dtbbpy)](PF$_6$) in ACN and 1 mL of a 1.00 mM solution of [Rh(dtbbpy)$_3$](PF$_6$)$_3$ in ACN. Concentrated to dryness by rotary evaporation soon thereafter. Immediately preceding photolysis, added 10 ml of a 0.6 M solution of TEA in the appropriate THF-D$_2$O-H$_2$O mixture (8:2:0, 8:1:1, 8:0:2). Evaluated according to the general photolysis procedure above and analyzed headspace by RGA. The endpoint results are included in the main text. The kinetic plots are presented below as Figure S6.

Photophysics Experimental Procedure and Results

Photophysics. Photophysical experiments were conducted at ambient temperature in a 1.0 cm screw-top quartz cuvette. UV-Vis absorption measurements were recorded using a Hewlett-Packard 8453 spectrometer equipped with a diode-array detector. Emission spectra were recorded using a Jobin-Yvon Fluorolog-3 spectrometer equipped with double monochromators and a Hamamatsu-928 photomultiplier tube (PMT) as the detector. To ensure the solutions were oxygen-free for luminscence measurements, the solution was bubbled with a solvent-saturated nitrogen stream for 10 min prior to measurement.

Quenching Studies. Dynamic quenching studies were conducted by measuring the emission lifetimes of deoxygenated solutions with 0.5 mM Ir-PS and a range of quencher concentrations. The samples were excited with an N$_2$ laser (Laser Science, Inc. VSL-337LRF, 10 ns pulse, 337 nm), and the emission decay was recorded using the emission monochromator, PMT detector, and a Tektronix TDS 3032B digital phosphor oscilloscope. Made a range of quencher concentrations by serial dilution of the stock quencher solutions with the non-quencher solutions as listed below. Bubbled an ACN- or THF-saturated stream of N$_2$ for 10 min prior to emission lifetime measurement. The data and Stern-Volmer analysis are presented below as Figure S10. For [Rh(dtbbpy)$_3$]$^{3+}$ quenching of [Ir(f-mppy)$_2$(dtbbpy)]$^{+*}$ in 80% THF-water, there is not a good Stern-Volmer fit because solubility issues for [Rh(dtbbpy)$_3$](PF$_6$)$_3$ limit the concentration range to an area where there is little quenching. For this reason, the value in 90% ACN-water is probably a more accurate indicator of the [Rh(dtbbpy)$_3$]$^{3+}$ quenching value in our system.

For TEA quenching of [Ir(ppy)$_2$(bpy)]$^{+*}$ in ACN prepared one stock solution that is 0.5 mM of [Ir(ppy)$_2$(bpy)](PF$_6$) in ACN and another stock solution that is 0.5 mM of [Ir(ppy)$_2$(bpy)](PF$_6$) and 90 mM of TEA in ACN.

For DMA quenching of [Ir(ppy)$_2$(bpy)]$^{+*}$ in ACN prepared one stock solution that is 0.5 mM of [Ir(ppy)$_2$(bpy)](PF$_6$) in ACN and another stock solution that is 0.5 mM of [Ir(ppy)$_2$(bpy)](PF$_6$) and 80 mM of DMA in ACN.

For TEA quenching of [Ir(f-mppy)$_2$(dtbbpy)]$^{+*}$ in 80% THF-water prepared one stock solution that is 0.5 mM of [Ir(f-mppy)$_2$(dtbbpy)](PF$_6$) in 80% THF-water and another stock solution that is 0.5 mM of [Ir(f-mppy)$_2$(dtbbpy)](PF$_6$) and 98.9 mM of TEA in 80% THF-water.

For [Rh(dtbbpy)$_3$]$^{3+}$ quenching of [Ir(f-mppy)$_2$(dtbbpy)]$^{+*}$ in 80% THF-water prepared one stock solution that is 0.5 mM of [Ir(f-mppy)$_2$(dtbbpy)](PF$_6$) in 80% THF-water and another stock solution that is 0.5 mM of [Ir(f-mppy)$_2$(dtbbpy)](PF$_6$) and 113 μM of [Rh(dtbbpy)$_3$](PF$_6$)$_3$ in 80% THF-water.

For [Rh(dtbbpy)$_3$]$^{3+}$ quenching of [Ir(f-mppy)$_2$(dtbbpy)]$^{+*}$ in 90% ACN-water prepared one stock solution that is 0.5 mM of [Ir(f-mppy)$_2$(dtbbpy)](PF$_6$) in 90% ACN-water and another stock solution that is 0.5 mM of [Ir(f-mppy)$_2$(dtbbpy)](PF$_6$) and 1 mM of [Rh(dtbbpy)$_3$](PF$_6$)$_3$ in 90% ACN-water.
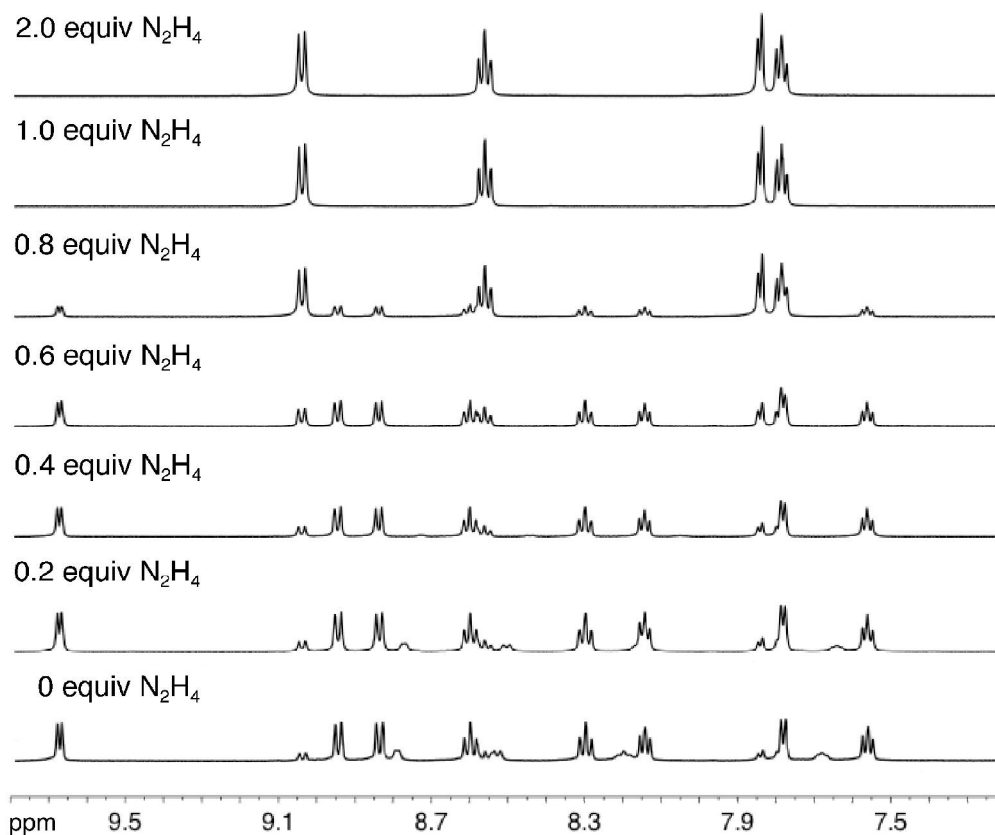
Figure S1. The NMR spectra of the aromatic region for the crude products in the N_2H_4 titration experiment
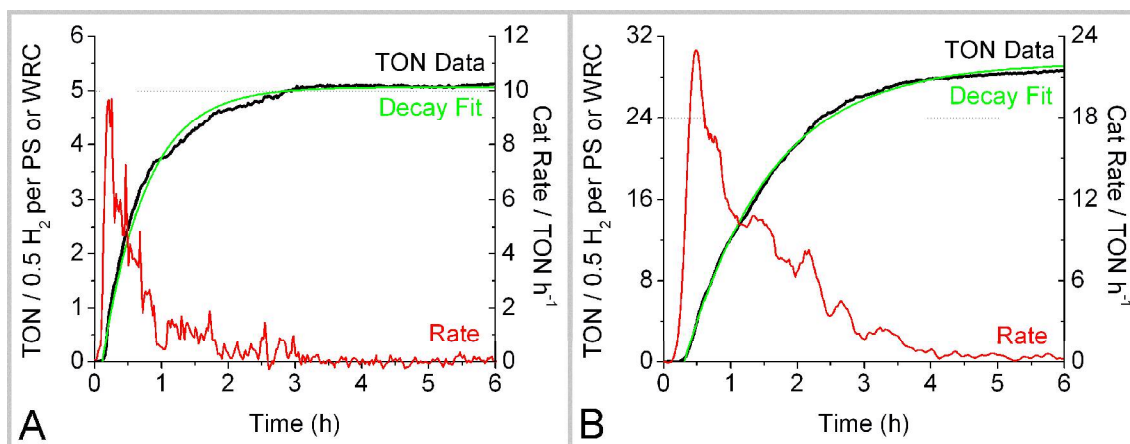

Figure S2: Unimolecular exponential decay fit and catalytic rate plot for the H_2-evolving photoreactions of the ER comparison study. Reaction conditions are 10 µmol of $[Ir(ppy)_2(bpy)](PF_6)$ and either $[Co(bpy)_3]Cl_2$ (Graph A) or $[Rh(bpy)_3](PF_6)_3$ (Graph B) with 10 mL of 0.6 M TEOA sol in 50% ACN-H_2O with continuous photolysis (500 mW, 465 nm) for 6 hours.
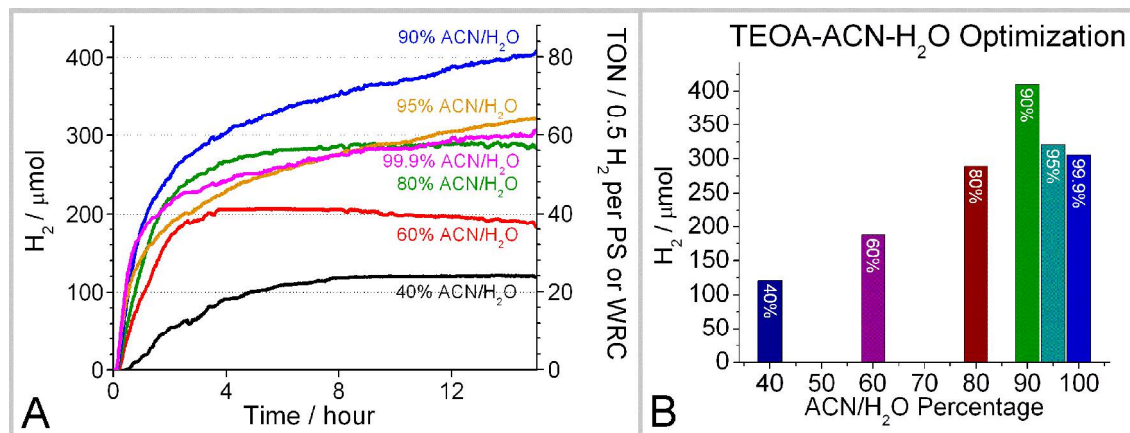
Figure S3: A) Kinetics traces and B) a graph illustrating endpoint results for the H_2-evolving photoreactions of the ACN-H_2O ratio study. Reaction conditions are 10 µmol of [Ir(ppy)$_2$(bpy)](PF$_6$) and [Rh(bpy)$_3$](PF$_6$)$_3$ with 10 mL of 0.6 M TEOA sol in 40%, 60%, 80%, 90%, 95%, or 100% ACN-H_2O with continuous photolysis (500 mW, 465 nm) for 15 hours.
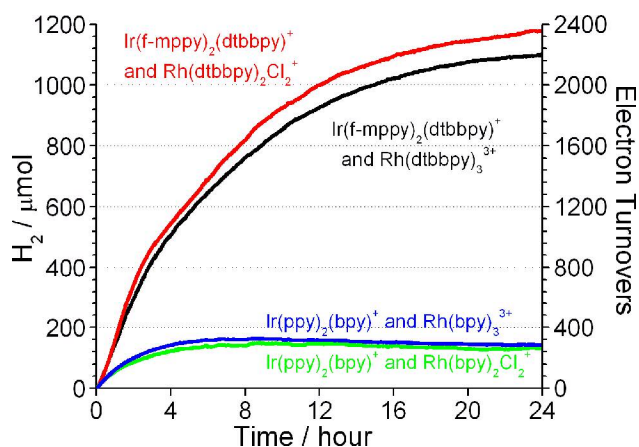

Figure S4: Evaluation of [Ir(C^N)$_2$(N^N)](PF$_6$) with [Rh(N^N)$_3$](PF$_6$)$_3$ or [Rh(N^N)$_2$Cl$_2$](PF$_6$) in photosynthetic-H_2 reactions (1 µmol of PS and WRC with 10 mL of 0.6 M TEA in 80% THF-H_2O, 460 nm, 500 mW, 24 h) where C^N and N^N are either f-mppy and dtbbpy or ppy and bpy.
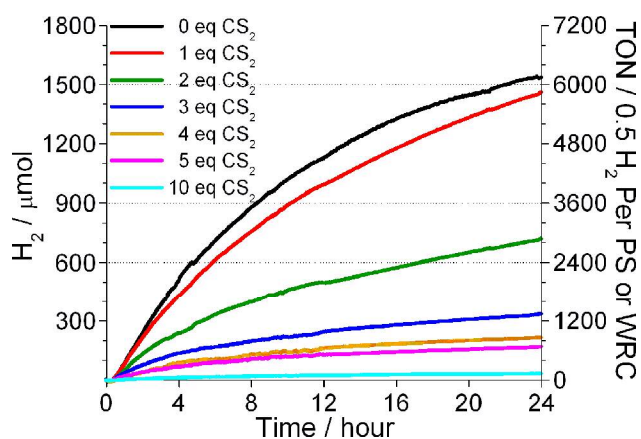
Figure S5: Evaluation of quantitative CS_2 poisoning of [Ir(f-mppy)$_2$(dtbbpy)](PF$_6$) and [Rh(dtbbpy)$_3$](PF$_6$)$_3$ in photosynthetic-H$_2$ reactions (0.5 µmol of PS and WRC with 10 mL of 0.6 M TEA in 80% THF-water, 460 nm, 500 mW, 24 h). Reactions include the appropriate amount of CS_2 (0, 0.5, 1, 1.5, 2, 2.5, or 5 µmol) as indicated on the graph.
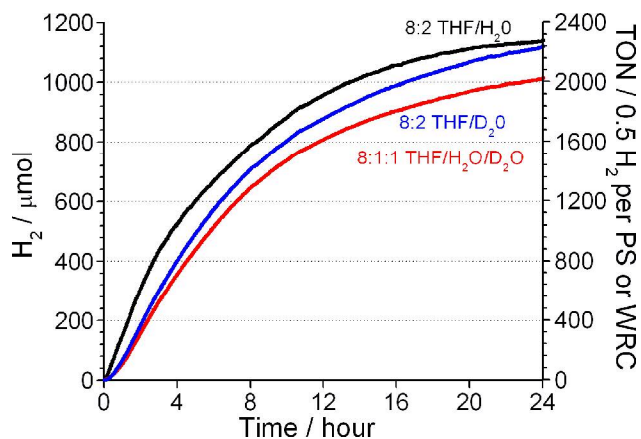

Figure S6: Evaluation of [Ir(f-mppy)$_2$(dtbbpy)](PF$_6$) and [Rh(dtbbpy)$_3$](PF$_6$)$_3$ in photosynthetic-H$_2$ reactions (1 µmol of PS and WRC with 10 mL of 0.6 M TEA in appropriate solvent, 460 nm, 500 mW, 24 h) where the media is 8:2 THF/H$_2$O, 8:2 THF/D$_2$O, or 8:1:1 THF/H$_2$O/D$_2$O.
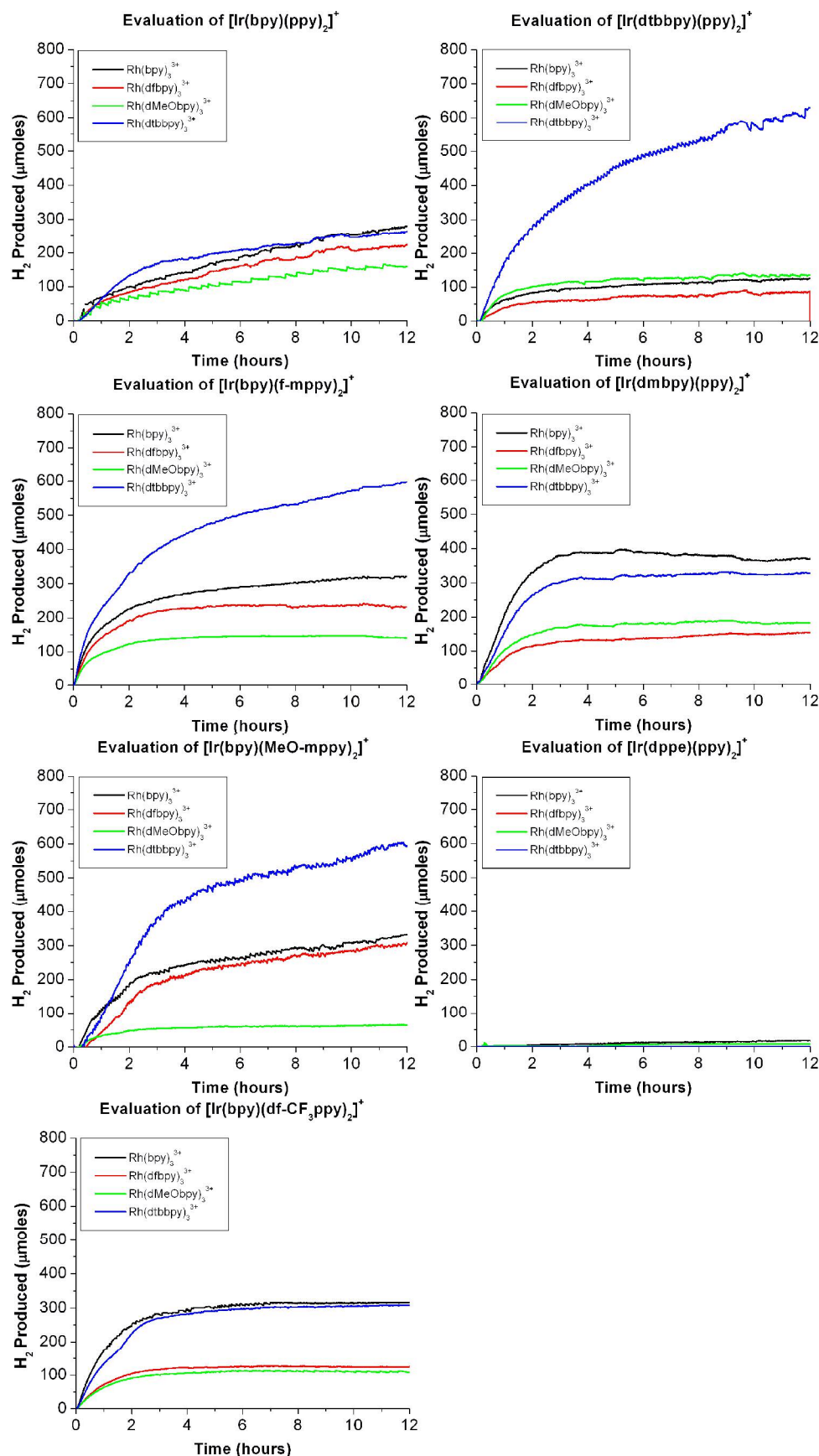
Figure S7: Kinetics traces for the H$_2$-evolving photoreactions of the combinatorial screening study. Reaction conditions are 10 µmol of PS and ER with 10 mL of 0.6 M TEOA sol in 90% ACN-H$_2$O with continuous photolysis (500 mW, 465 nm) for 12 hours. The PS is listed in the chart title and the ER for each data series is indicated in the chart legend.
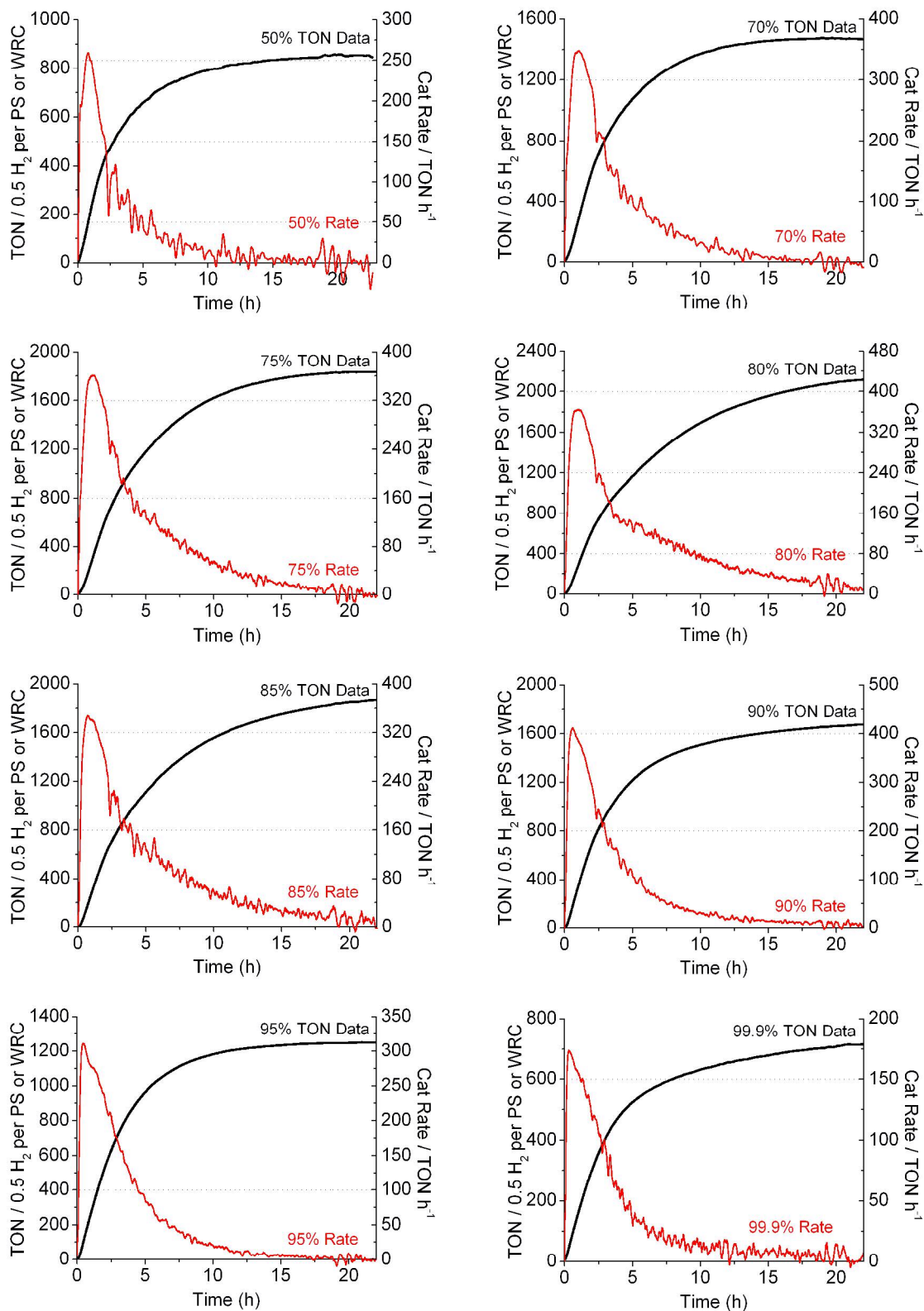
Figure S8: Kinetics and catalytic rate plots for [Ir(f-mppy)$_2$(dtbbpy)](PF$_6$) and [Rh(dtbbpy)$_3$](PF$_6$)$_3$ in photosynthetic-H$_2$ reactions (1 µmol of PS and WRC with 10 mL of 0.6 M TEA in appropriate solvent mixture, 460 nm, 500 mW, 22 h) where the solution is 50, 70, 75, 80, 85, 90, 95, or 99.9% THF-H$_2$O.
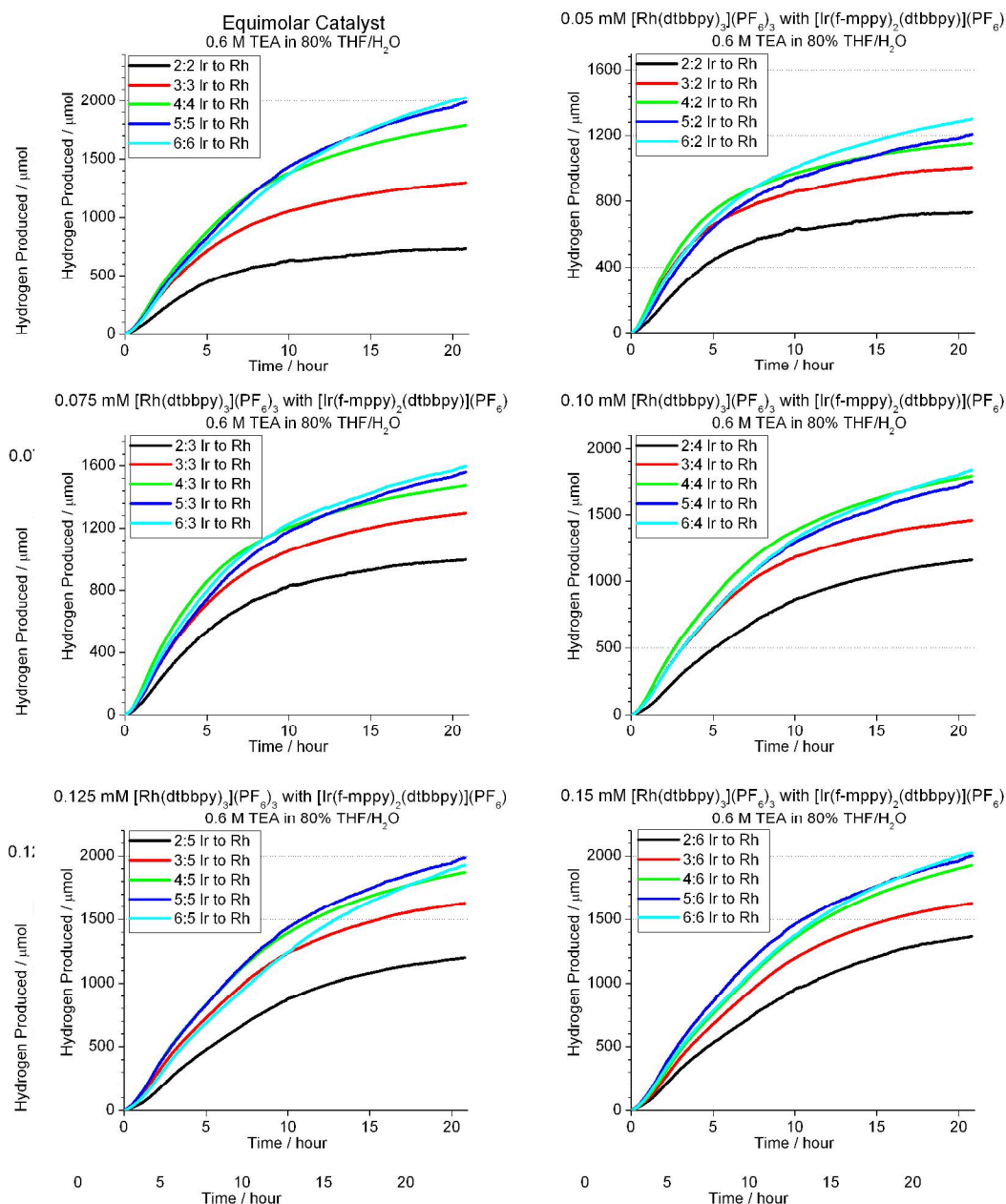
Figure S9: Kinetics plots for $[Ir(f\text{-}mppy)_2(dtbbpy)](PF_6)$ and $[Rh(dtbbpy)_3](PF_6)_3$ in photosynthetic-H_2 reactions (0.5 to 1.5 µmol of PS and WRC with 10 mL of 0.6 M TEA in 80% THF-water, 460 nm, 500 mW, 22 h) with varying catalyst concentration and ratios as indicated in the graphs.

[Ir(ppy)$_2$(bpy)](PF$_6$) with TEA
in 100% ACN

[Quencher] (M)	τ (ns)	error (ns)	τ_0/τ	error
0.54	15.1	0.094	26.09272	0.175413
0.36	21.5	0.092	18.32558	0.091173
0.18	41.26	0.097	9.5492	0.033036
0	394	1	1	0.003589

slope	47.5 M^{-1}
kq	1.21E+08 M^{-1}s^{-1}
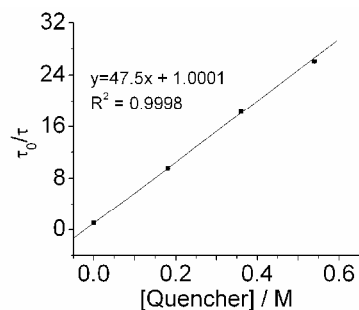
[Ir(ppy)$_2$(bpy)](PF$_6$) with DMA
in 100% ACN

[Quencher] (M)	τ (ns)	error (ns)	τ_0/τ	error
0.008	21	0.1	18.75714	0.111456
0.0008	144.3	0.2	2.72973	0.010414
0.00008	329	0.4	1.197264	0.004497
0	393.9	1.4	1	0.005026

slope	2219.1 M^{-1}
kq	5.63E+09 M^{-1}s^{-1}
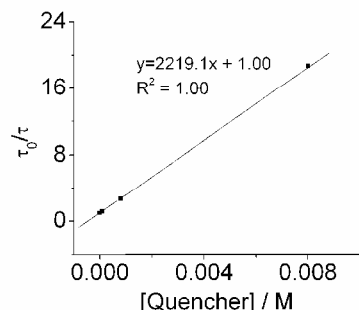
[Ir(f-mppy)$_2$(dtbbpy)](PF$_6$) with TEA
in 80% THF-water

[Quencher] (M)	τ (ns)	error (ns)	τ_0/τ	error
0.09892	0.133	0.0001	8.631579	0.026375
0.04946	0.241	0.0012	4.763485	0.027597
0.00989	0.673	0.0021	1.705795	0.007339
0.00495	0.796	0.0024	1.442211	0.006095
9.89E-04	1.063	0.0025	1.079962	0.004084
4.95E-04	1.092	0.0032	1.051282	0.00438
9.89E-05	1.145	0.0026	1.00262	0.003742
0	1.148	0.0034	1	0.004188

slope	76.92 M^{-1}
kq	6.70E+07 M^{-1}s^{-1}
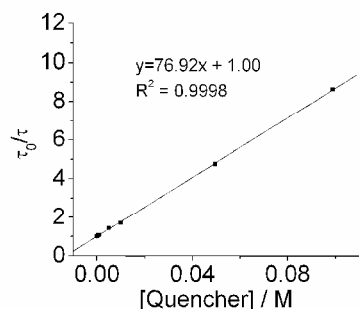
[Ir(f-mppy)$_2$(dtbbpy)](PF$_6$) with [Rh(dtbbpy)$_3$](PF$_6$)$_3$
in 80% THF-water

[Quencher] (M)	τ (ns)	error (ns)	τ_0/τ	error
0.000113	1.13	0.003	1.015929	0.003785
5.65E-05	1.142	0.004	1.005254	0.004393
1.13E-05	1.144	0.003	1.003497	0.003715
5.65E-06	1.15	0.003	0.998261	0.003686
1.13E-06	1.143	0.003	1.004374	0.00372
0	1.148	0.003	1	0.003696

slope	132.21 M^{-1}
kq	1.15E+08 M^{-1}s^{-1}
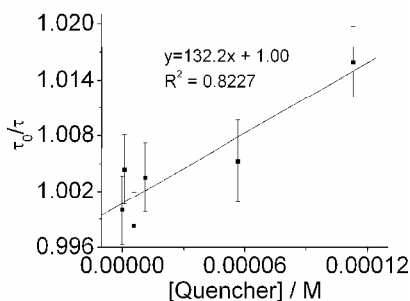
[Ir(f-mppy)$_2$(dtbbpy)](PF$_6$) with [Rh(dtbbpy)$_3$](PF$_6$)$_3$
in 90% ACN-water

[Quencher] (M)	τ (ns)	error (ns)	τ_0/τ	error
0.001	1320		1.093182	
0.0008	1345		1.072862	
0.0006	1363		1.058694	
0.0004	1390		1.038129	
0.0002	1415		1.019788	
0	1443		1	

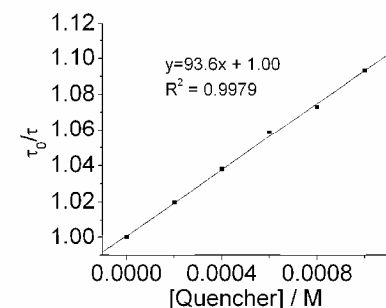|	
slope	93.6 M^{-1}
kq	6.49E+07 M^{-1}s^{-1}

Figure S10. Stern-Volmer analysis of dynamic quenching for the Ir-PSs and Quenchers indicated in the figure.

Table S1. Endpoint results, max catalytic rates, and quantum yields for varying ratios and concentrations of [Ir(f-mppy)$_2$(dtbbpy)](PF$_6$) and [Rh(dtbbpy)$_3$](PF$_6$)$_3$ in photosynthetic-H$_2$ reactions (10 mL of 0.6 M sol of TEA in 80% THF-H$_2$O, 460 nm, 500 mW, 20 h) range from 0.05 to 0.15 mM, as indicated.

Ir Conc (μM)	Rh Conc (μM)	H$_2$ (μmol)	Ir TON	Rh TON	Max Φ (1/2 H$_2$)	Ir Max Rate (TON/h)	Rh Max Rate (TON/h)
50	50	736	2944	2944	0.28	459	459
50	75	997	3988	2659	0.34	560	373
50	100	1161	4644	2322	0.32	528	264
50	125	1201	4804	1922	0.30	494	198
50	150	1368	**5472**	1824	0.34	**563**	188
75	50	1007	2685	4028	0.32	520	779
75	**75**	**1298**	**3461**	**3461**	**0.32**	**521**	**521**
75	100	1461	3896	2922	0.33	535	402
75	125	1631	4349	2610	0.31	499	299
75	150	1629	4344	2172	0.30	483	242
100	50	1152	2304	4608	0.28	442	**884**
100	75	1475	2950	3933	0.31	484	645
100	100	1788	3576	3576	0.31	476	476
100	125	1872	3744	2995	0.29	447	357
100	150	1927	3854	2569	0.26	409	273
125	50	1207	1931	4828	0.18	269	672
125	75	1560	2496	4160	0.21	318	530
125	100	1747	2795	3494	0.22	327	409
125	125	1987	3179	3179	0.23	354	354
125	150	2002	3203	2669	0.24	364	303
150	50	1299	1732	**5196**	0.17	252	757
150	75	1598	2131	4261	0.19	285	569
150	100	1832	2443	3664	0.18	268	401
150	125	1928	2571	3085	0.16	235	282
150	150	2027	2703	2703	0.18	271	271